onco

MDPI

Article

Assessment of a Nano-Docetaxel Combined Treatment for Head and Neck Cancer

Gee Young Lee [1,2], Mohamed Mubasher [3], Tamra S. McKenzie [4], Nicole C. Schmitt [5], Merry E. Sebelik [4,5], Carrie E. Flanagan [4,5], Badi El Osta [4,6], Maya B. Cothran [7] and Hadiyah-Nicole Green [1,2,7,*]

1 Department of Surgery, Morehouse School of Medicine, 720 Westview Drive, Atlanta, GA 30310, USA; glee@msm.edu
2 Biomedical Laboratory Research & Development Service, Department of Veterans Affairs, Office of Research and Development, Birmingham VA Medical Center, 700 19th Street, Birmingham, AL 35233, USA
3 Community Health and Preventive Medicine, Morehouse School of Medicine, 720 Westview Drive, Atlanta, GA 30310, USA; mmubasher@msm.edu
4 Atlanta VA Medical Center, Atlanta VA Health Care System, 1670 Clairmont Road, Decatur, GA 30033, USA; Tamra.McKenzie-Johnson@va.gov (T.S.M.); merry.sebelik@emory.edu (M.E.S.); Carrie.Flanagan@va.gov (C.E.F.); badi.elosta@emoryhealthcare.org (B.E.O.)
5 Department of Otolaryngology-Head and Neck Surgery, Emory University School of Medicine, 550 Peachtree Road NE, Atlanta, GA 30308, USA; nicole.cherie.schmitt@emory.edu
6 Department of Hematology and Medical Oncology, Winship Cancer Institute, Emory University School of Medicine, 1365 E Clifton Rd NE, Building C, Atlanta, GA 30322, USA
7 Ora Lee Smith Cancer Research Foundation, Advanced Technology and Development Center, 75 5th Street NW, Atlanta, GA 30308, USA; maya@oralee.org
* Correspondence: hgreen@msm.edu or drgreen@oralee.org; Tel.: +1-(205)-538-1283

Abstract: Objective: The combination of docetaxel (DTX) with Laser-Activated NanoTherapy (LANT), as a treatment for head and neck cancer (HNC), may enhance the therapeutic efficacy of lower doses of DTX, thereby minimizing the effective dosage, side effects and treatment times. Material and methods: Three HNSCC cell lines, Detroit 562, FaDu, and CAL 27, were treated with four combinations of DTX + LANT to evaluate DTX dose reduction and cell viability. Results: The 1 nM DTX + 5 nM LANT combination was the most effective treatment, increasing cell death over its corresponding DTX monotreatment with approximately 86.6%, 80.7%, and 92.1% cell death for Detroit 562, FaDu, and CAL 27, respectively. In Detroit 562, the 1 nM DTX + 5 nM LANT combination treatment resulted in the highest percentage of DTX dose reduction at 84.6%; in FaDu and CAL 27, the 0.5 nM DTX + 5 nM LANT combination treatment resulted in the highest percentage of DTX dose reduction at 78.2% and 82.4%, respectively. Conclusion: LANT may increase the therapeutic efficacy of DTX at significantly lower doses, which could improve patient outcomes.

Keywords: docetaxel; combination therapy; nanoparticles; head and neck squamous cell carcinoma; oncology; therapies

Citation: Lee, G.Y.; Mubasher, M.; McKenzie, T.S.; Schmitt, N.C.; Sebelik, M.E.; Flanagan, C.E.; Osta, B.E.; Cothran, M.B.; Green, H.-N. Assessment of a Nano-Docetaxel Combined Treatment for Head and Neck Cancer. *Onco* **2021**, *1*, 83–94. https://doi.org/10.3390/onco1020007

Academic Editor: Steven A. Rosenzweig

Received: 24 July 2021
Accepted: 18 September 2021
Published: 29 September 2021

1. Introduction

Head and neck cancers (HNC) have a poor prognosis with a worldwide 5-year survival rate of less than 50% [1–3], and head and neck squamous cell carcinomas (HNSCC) constitute 90% of these cases [4]. Many HNC patients present with locally advanced, difficult-to-treat, inoperable, recurrent, or drug-resistant tumors [1–7]. Docetaxel (DTX) is an anticancer drug that disrupts normal microtubule functioning during the cell cycle. It inhibits interphase and mitosis by promoting and stabilizing the microtubule assembly that prevents microtubule depolymerization, making the G2/M transition impossible [8,9]. This mechanism limits cell growth in the locoregional area of the tumor. However, DTX is associated with adverse effects that may be severe or dose-limiting, including febrile neutropenia, neuropathy, and alopecia [10–17]. Better patient outcomes may be achieved with lower DTX doses that would result in fewer severe side effects.

The scientific community is beginning to explore strategies to shift the therapeutic window and reduce the effective dose of DTX. These strategies may limit complications by combining DTX with other treatment modalities and manipulating the dosing schedule [5,7]. For locally advanced HNSCC, DTX is paired concurrently with other chemotherapeutic drugs. The established dose for this cancer type is 75 mg/m^2 when administered with cisplatin and fluorouracil at varying dosages and schedules, depending on the subsequent treatments such as radiation or chemotherapy [18–21]. Studies combining DTX with other chemotherapeutic drugs and varying the DTX dosage and delivery have shown great potential in decreasing side effects [19,22,23].

Nanoparticles and nanomaterials have shown to be promising anticancer therapeutics alone and in combination with chemotherapeutic agents. These nanomedicines have dramatically improved tumor targeting and therapeutic efficacy when used in drug delivery systems, radiotherapy, and photothermal or photodynamic therapy [24–30]. Many nano-based approaches have been combined with DTX to enhance targeted drug delivery and tumor specificity, consequently minimizing side effects [23,31–37]. Photothermal therapies utilizing nanoparticles and laser light have shown success in tumor treatment in vitro and in vivo as a site-specific ablative approach rather than theranostic drug delivery [37,38]. Our work focuses on a particular class of laser-activated nanoparticles, specifically, a thermal ablation platform treatment using near-infrared excitation of gold nanorods (AuNRs), known as Laser-Activated NanoTherapy (LANT) (Figure 1). This LANT platform is not designed to enhance targeting but specifically to induce locoregional cell death at the site of laser activation for the sole purpose of its thermal ablation and therapeutic effect. Our prior work with LANT as a single modality has demonstrated ~100% cell death in vitro ($p < 0.0001$) and ~100% tumor regression in vivo ($p < 0.0001$) with no observable side effects [39,40]. However, to our knowledge, no such platform has been approved by the United States Food and Drug Administration (FDA) for use in humans. LANT presents an opportunity to override some of the physiologic obstacles encountered within the tumor microenvironment and with DTX specificity that lead to severe side effects when using the current DTX dosing schedule. The present study investigates how LANT may enhance the therapeutic efficacy of lower doses of DTX for treating three head and neck squamous cell carcinoma (HNSCC) cell lines.

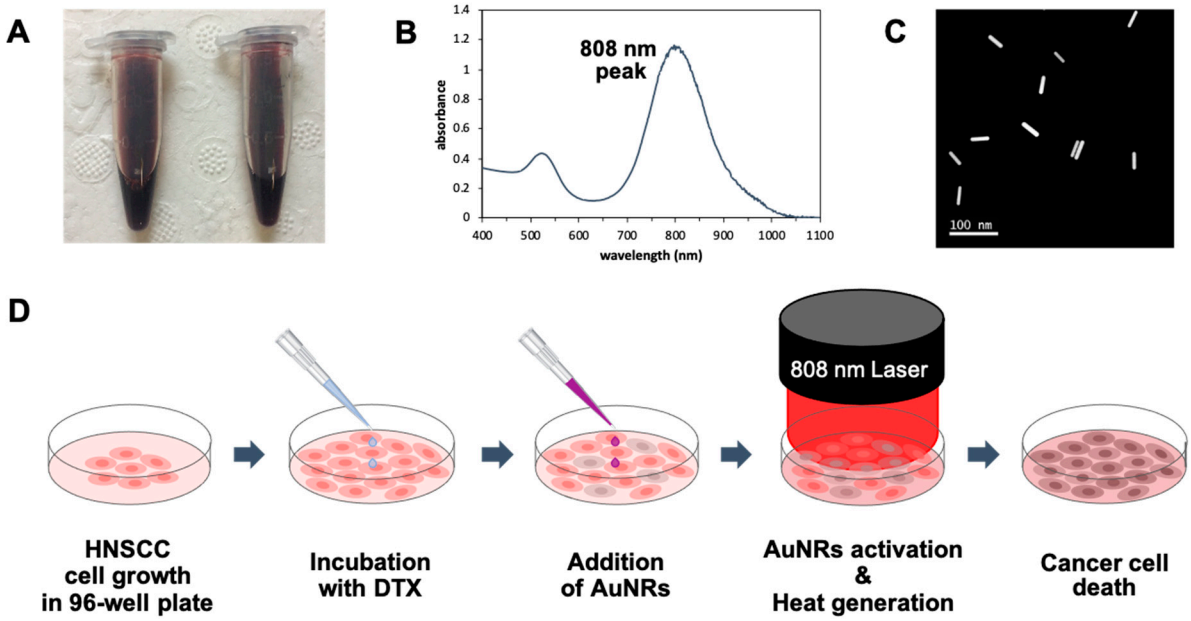

Figure 1. (**A**) PEGylated AuNRs solution utilized in Laser-Activated Nanotherapy (LANT); (**B**) UV-VIS-NIR spectrum of AuNRs showing an 808 nm absorption peak and (**C**) scanning transmission electron microscope (STEM) image of AuNRs having 40 nm in length, 10 nm in width, and aspect ratio (R = 4), with up to six-month stability; and (**D**) schematic illustration of DTX and LANT combination treatment in vitro. The illustration demonstrates one well of a 96-well plate.

2. Results

2.1. Cell Death Effects of LANT Monotreatment

The in vitro effects of LANT as a monotreatment (percentage of cell death, dose-response curves, and half-maximal effective concentrations (EC50) of 8.1, 11.0, and 6.7 nM) were previously established for Detroit 562, FaDu, and CAL 27, respectively [41,42]. In summary, 4 min NIR laser excitation of AuNRs at six concentrations (0, 5, 10, 15, 20, and 25 nM) demonstrates AuNR concentration-dependent cell death (Figure 2). LANT induced significant cell death in all three HNSCC cell lines with increasing AuNR concentration, directly increasing the percentage of cell death. Consistent with our previous findings [39], LANT doses of 25 nM induced approximately 100% cell death ($p < 0.0001$) in all three HNSCC cell lines.

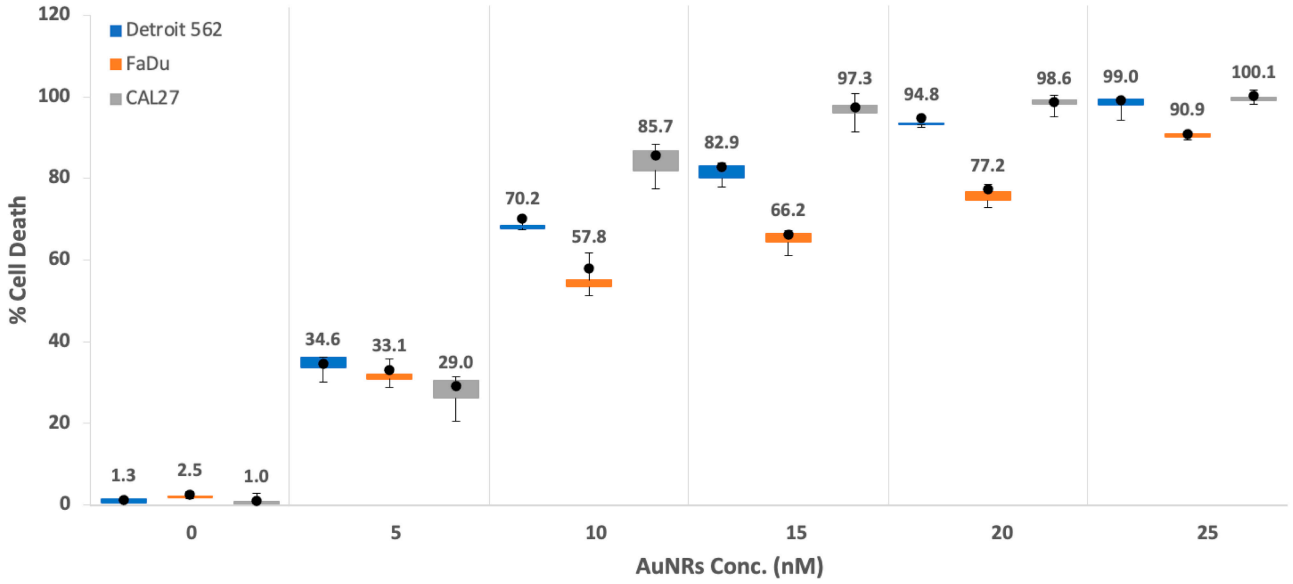

Figure 2. Box and Whisker plot to display LANT monotreatment dose-response with AuNRs concentration for HNSCC cell lines: Detroit 562 (blue box), FaDu (orange box), and CAL 27 (gray box) at concentrations of 0, 5, 10, 20, and 25 nM; 25 µL of AuNRs per well, with and without 808 nm NIR activation for 4 min at 1.875 W/cm^2. Dots show the mean values of $n = 6$.

2.2. Cell Death Effects of DTX Monotreatment

To establish dose–response curves and EC50 for DTX monotreatment, the percentage of cell death induced was determined after incubating the cells for 48-h with DTX concentrations ranging between 0.0025–20 nM, resulting in a dose-dependent increase in cell death (Figure 3). Detroit 562 and FaDu were more sensitive to DTX at lower doses (1 nM and lower), whereas CAL 27 was most responsive to DTX at higher doses (2.5 nM and higher). The EC50 values of DTX for Detroit 562, FaDu, and CAL 27 were 1.09, 0.90, and 1.24 nM, respectively (Table 1). In the present study, 20 nM of DTX resulted in approximately 94% cell death in Detroit 562 and FaDu and greater than 99% cell death in CAL 27 48 h after treatment.

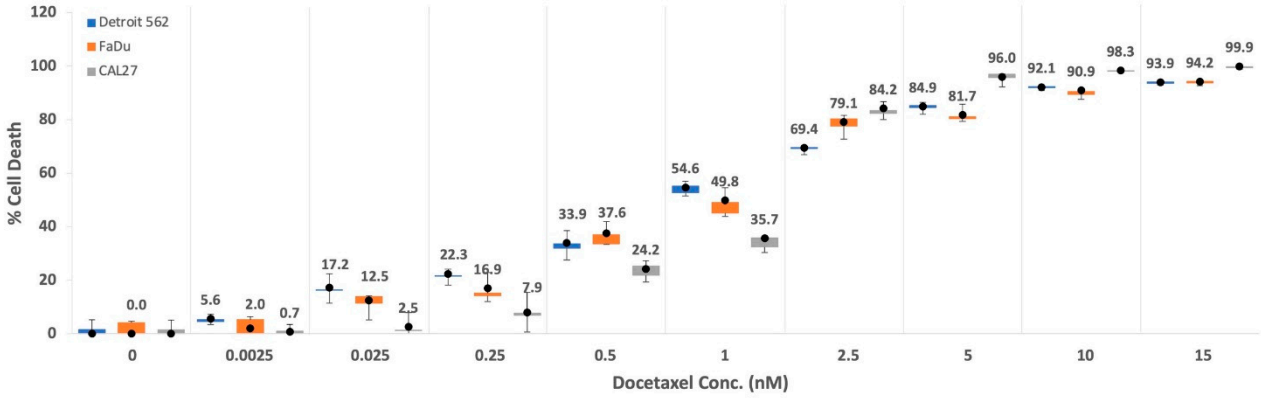

Figure 3. Box and Whisker plot to display DTX monotreatment dose-response with DTX concentration for HNSCC cell lines: Detroit 562 (blue box), FaDu (orange box), and CAL 27 (gray box). Mean percentage of cell death induced by a 48-h incubation with DTX as a monotreatment at 9 different concentrations of 0.0025, 0.025, 0.25, 0.5, 1, 2.5, 5, 10, and 15 nM for each cell line. Dots show the mean values of $n = 6$.

Table 1. EC50 values for LANT and DTX monotreatments. The EC50 values informed the AuNRs concentrations and DTX doses used in the combination treatment.

EC50	Cell Lines		
	Detroit 562	**FaDu**	**CAL 27**
LANT (nM)	8.08	11.03	6.68
DTX (nM)	1.09	0.90	1.24

2.3. Combination of DTX and LANT Treatments, Synergy, and Dose Reduction

The monotreatment EC50 values that induced 50% cell death (Table 1) informed the dose selection for the combination experiments to narrow the focus to low doses of DTX and LANT. To delineate the efficacy of the DTX + LANT combination treatment, 0.5 and 1 nM of DTX were selected for the combination treatment as these concentrations induced less than 50% cell death for all cell lines. Likewise, 2.5 and 5 nM of AuNRs for LANT were selected as these concentrations induced less than 50% cell death for all cell lines. The percentage of DTX dose reduction was determined using the 4PL model equations according to our previously described methods [43,44]. In short, using the 4PL model equations of DTX monotreatment for each cell line (Equations (1)–(3)) and the cell death percentage induced by the DTX and LANT combination, we calculated the corresponding DTX monotreatment dose necessary to achieve the same cell death and finally, the percentages of DTX dose reduction shown in Table 2.

We define synergy as when the percentage of cell death induced by the combination treatment of DTX + LANT is greater than the sum of the individual monotreatment-induced percentages of cell death. The mean percentage of cell death generated by combining low dose DTX and low dose LANT was greater than DTX monotreatment, and a synergistic effect was observed in most instances (Figure 4). In particular, the percentage of cell death due to the three DTX + LANT combination treatments, 0.5 nM DTX + 5 nM LANT (Figure 4B), 1 nM DTX + 2.5 nM LANT (Figure 4C), and 1 nM DTX + 5 nM LANT (Figure 4D) was significantly higher than the two DTX monotreatments (0.5 or 1 nM) or two LANT monotreatments (2.5 or 5 nM) for all three HNSCC cell lines, Detroit 562, FaDu, and CAL 27. For example, in the case of CAL 27 shown in Figure 4B, the percentage of cell death by 0.5 nM DTX + 5 nM LANT combination treatment, 84.1% was much greater than the summation of each percentage by 0.5 nM DTX and 5 nM LANT monotreatments, 63.9% (34.9% + 29.0%). The therapeutic efficacy of low-dose DTX combined with LANT leads to a DTX dose reduction (Table 2). For Detroit 562, the largest DTX dose reduction was achieved by 1 nM DTX + 5 nM LANT combination treatment: 84.6%. The 0.5 nM DTX + 5 nM LANT

combination treatment resulted in the highest percentage of DTX dose reduction for FaDu and CAL 27: 78.2% and 82.4%, respectively. For example, 86.6% Detroit 562 cell death can be induced by 6.5 nM of DTX monotreatment or 1 nM DTX when combined with 5 nM LANT, demonstrating an 84.6% DTX dose reduction.

Table 2. DTX dose reduction percentage by DTX + LANT combination treatment.

Cell Line	Outcome	Treatment Combination			
		0.5 nM DTX + 2.5 nM LANT	**0.5 nM DTX + 5 nM LANT**	**1 nM DTX + 2.5 nM LANT**	**1 nM DTX + 5 nM LANT**
Detroit 562	Cell death (%) in combo	48.4	57.5	81.3	86.6
	Est. conc. (nM) of DTX mono to obtain the same % cell death	0.9	1.3	4.4	6.5
	DTX dose reduction (%)	43.0	61.7	77.2	84.6 [a]
FaDu	Cell death (%) in combo	40.9	73.1	67.0	80.6
	Est. conc. (nM) of DTX mono to obtain the same % cell death	0.6	2.3	1.7	3.5
	DTX dose reduction (%)	22.7	78.2 [a]	42.2	71.5
CAL 27	Cell death (%) in combo	49.0	84.1	80.9	92.1
	Est. conc. (nM) of DTX mono to obtain the same % cell death	1.2	2.8	2.6	4.2
	DTX dose reduction (%)	57.0	82.4 [a]	60.8	76.0

[a] Indicates the combination treatment that resulted in the highest percentage of DTX dose reduction for each cell line.

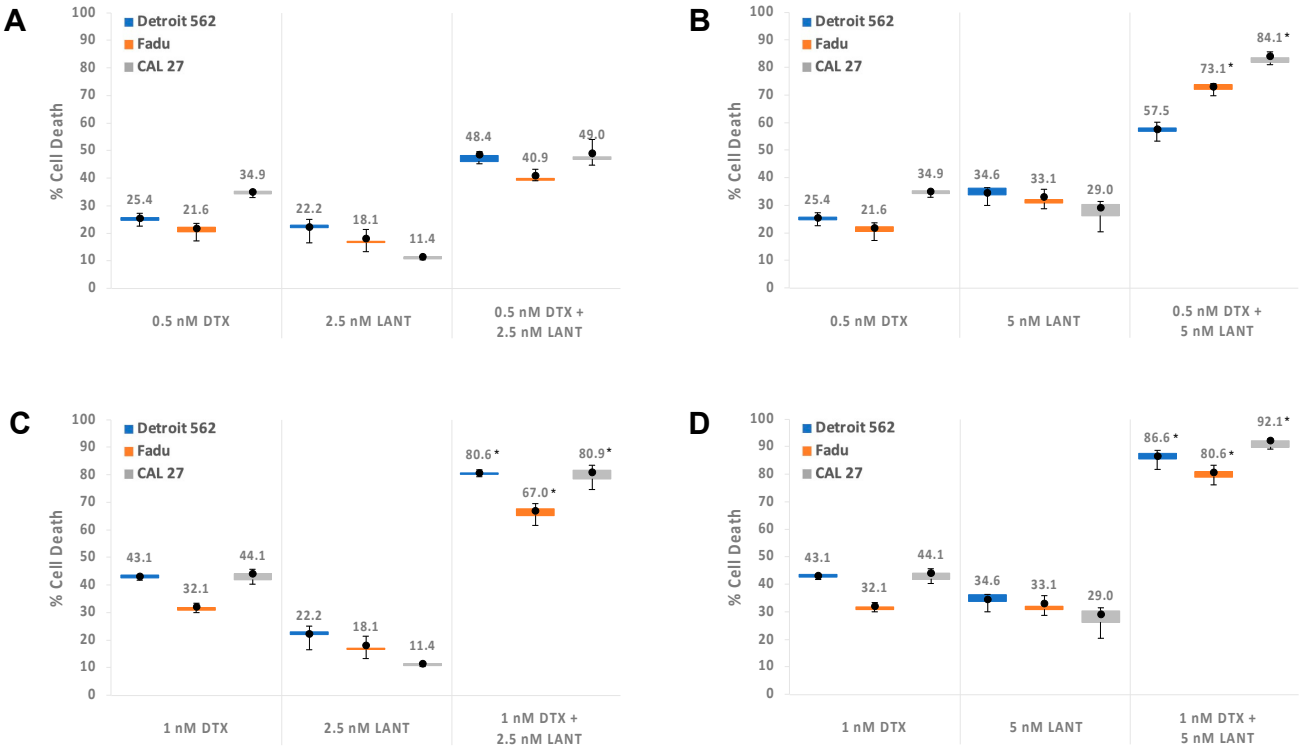

Figure 4. Box and Whisker plot to display the synergy of LANT and DTX combination treatment for HNSCC cell lines: Detroit 562 (blue bar), FaDu (orange bar), and CAL 27 (gray bar). (**A**) 0.5 nM DTX + 2.5 nM LANT combination, (**B**) 0.5 nM DTX + 5 nM LANT combination, (**C**) 1 nM DTX + 2.5 nM LANT combination, and (**D**) 1 nM DTX + 5 nM LANT combination. Cells were subjected to a 48-h incubation with 0.5 or 1 nM DTX and 4-min exposure of 2.5 or 5 nM LANT as a monotreatment or combination; NIR laser excitation for 4 min at 1.875 W/cm^2. Dots show the mean values of n = 4 and * indicates synergic effect.

2.4. Summary Statistics and Linear Mixed Model (LMM) Regression Post Hoc Results

According to our previously established methods, the LMM regression post hoc test compared the means of the six DTX and LANT monotreatments versus combination treatment groups for all three HNSCC cell lines [42]. These post hoc analyses are summarized in Table 3, showing statistically significant differences ($p < 0.05$) in the means for most of the comparison groups. DTX and LANT treatment combinations were, in general, significantly more effective than the corresponding DTX monotreatments. In this study, the best-performing treatment regimen combined 1 nM DTX + 5 nM LANT, with approximately an 86.6%, 80.6%, and 92.1% increase in cell death versus 1 nM DTX alone for Detroit 562, FaDu, and CAL 27 cells, respectively. The other treatment combinations also induced significantly more cell death than 0.5 or 1 nM DTX alone. There were two comparisons (of 15 comparisons) for Detroit 562 and CAL 27 and 1 comparison for FaDu that did not reach statistical significance (Table 3). The LANT monotreatment was omitted from this comparison because we previously showed that the effective LANT monotreatment dose significantly induced tumor regression by approximately 100% ($p < 0.0001$) with no observed toxicity or side effects [39].

Table 3. Therapeutic efficacy comparison of 15 treatment groups.

Treatment Group Comparison [a] (First Column vs. Second Column)		Detroit 562			FaDu			CAL 27		
		Mean Diff. [b]	Unadj. *p*-Value [c]	Adj. *p*-Value [d]	Mean Diff. [b]	Unadj. *p*-Value [c]	Adj. *p*-Value [d]	Mean Diff. [b]	Unadj. *p*-Value [c]	Adj. *p*-Value [d]
0.5 nM DTX + 2.5 nM LANT	0.5 nM DTX	23.0	<0.0001 *	<0.0001 *	19.3	<0.0001 *	<0.0001 *	14.2	<0.0001 *	<0.0001 *
0.5 nM DTX + 5 nM LANT	0.5 nM DTX	32.1	<0.0001 *	<0.0001 *	51.5	<0.0001 *	<0.0001 *	49.2	<0.0001 *	<0.0001 *
1 nM DTX + 2.5 nM LANT	0.5 nM DTX	55.2	<0.0001 *	<0.0001 *	45.3	<0.0001 *	<0.0001 *	46.1	<0.0001 *	<0.0001 *
1 nM DTX + 5 nM LANT	0.5 nM DTX	61.1	<0.0001 *	<0.0001 *	59.0	<0.0001 *	<0.0001 *	57.3	<0.0001 *	<0.0001 *
0.5 nM DTX + 2.5 nM LANT	1 nM DTX	5.3	0.0219	0.3285	8.8	0.0002 §	0.0036 §	4.9	0.0306	0.4595
0.5 nM DTX + 5 nM LANT	1 nM DTX	14.4	<0.0001 *	<0.0001 *	41.0	<0.0001 *	<0.0001 *	40.0	<0.0001 *	<0.0001 *
1 nM DTX + 2.5 nM LANT	1 nM DTX	37.5	<0.0001 *	<0.0001 *	34.8	<0.0001 *	<0.0001 *	36.9	<0.0001 *	<0.0001 *
1 nM DTX + 5 nM LANT	1 nM DTX	43.4	<0.0001 *	<0.0001 *	48.5	<0.0001 *	<0.0001 *	48.1	<0.0001 *	<0.0001 *
1 nM DTX	0.5 nM DTX	17.7	<0.0001 *	<0.0001 *	10.5	<0.0001 *	0.0003	9.2	0.0001 §	0.0019 §
0.5 nM DTX + 5 nM LANT	0.5 nM DTX + 2.5 nM LANT	9.1	0.0001 §	0.0021 §	32.2	<0.0001 *	<0.0001 *	35.0	<0.0001 *	<0.0001 *
1 nM DTX + 2.5 nM LANT	0.5 nM DTX + 2.5 nM LANT	32.2	<0.0001 *	<0.0001 *	26.0	<0.0001 *	<0.0001 *	31.9	<0.0001*	<0.0001 *
1 nM DTX + 5 nM LANT	0.5 nM DTX + 2.5 nM LANT	38.2	<0.0001 *	<0.0001 *	39.7	<0.0001 *	<0.0001 *	43.1	<0.0001 *	<0.0001 *
1 nM DTX + 2.5 nM LANT	0.5 nM DTX + 5 nM LANT	23.1	<0.0001 *	<0.0001 *	−6.2	0.0077	0.1157	−3.1	0.1658	0.999
1 nM DTX + 5 nM LANT	0.5 nM DTX + 5 nM LANT	29.0	<0.0001 *	<0.0001 *	7.5	0.0014 †	0.0204 †	8.1	0.0006 †	0.0097 †
1 nM DTX + 5 nM LANT	1 nM DTX + 2.5 nM LANT	5.9	0.0101	0.1522	13.7	<0.0001 *	<0.0001 *	11.2	<0.0001 *	<0.0001 *

[a] Comparing the therapeutic efficacy of each DTX monotreatment and combination treatment groups by the Linear Mixed Model (LMM) regression post hoc tests with Bonferroni correction for three HNSCC cell lines. For treatment group comparison, the first column was more effective than the second column by the mean difference amount. [b] Mean Diff., Mean Difference = first column–second column [c] Unadj. *p*-value, unadjusted *p*-value; * $p < 0.0001$; § $p < 0.005$; and † $p < 0.05$ [d] Adj. *p*-value, adjusted *p*-value; * $p < 0.0001$; § $p < 0.005$; and † $p < 0.05$.

3. Discussion

Adjuvant, neoadjuvant, and combination therapies are emerging and viable approaches to overcome the current challenges experienced by patients who cannot receive or tolerate standard chemotherapeutic treatment regimens. This current in vitro study presents the possibility of a patient-centered solution that may reduce the standard DTX dosage and associated side effects for patients with locally advanced HNSCC. DTX has shown promise to decrease toxicity at lower doses when combined with other therapeutic interventions while maintaining or improving efficacy.

The most widely accepted DTX combination therapy for HNSCC patients is with cisplatin and 5-fluorouracil (TPF) [20,21]. This combination was found to effectively extend the survival rate in patients diagnosed with locally advanced HNSCC compared to cisplatin or cisplatin/5-fluorouracil (PF) alone [20,22]. Albers et al. demonstrated an effective and tolerable dosage of 75 mg/m^2 DTX on a 21-day cycle when combined with PF, a 25% decrease from the maximum tolerated dose of DTX as a single agent [45]. Other studies reveal improved outcomes with DTX dosage reduction, including a phase II clinical trial using DTX at 20 mg/m^2 per week combined with bevacizumab and radiotherapy. This combination showed promising survival outcomes despite a 40% decrease from the maximum standard dose of DTX [46]. Combining DTX with immune checkpoint inhibitors in HNSCC is also very promising [47].

Emerging preclinical and clinical studies combining DTX with novel interventions, such as nanomedicines and therapeutic nanotechnologies, offer a renewed potential for DTX dose reduction and enhanced drug delivery [23,31–37,48,49]. A variety of nanomaterials have impacted DTX effectiveness by allowing for selective distribution to the cancer cells, increased circulation times, and a more sustained drug release [32–34]. Furthermore, surface-coated nanoparticles may significantly increase targeting, decrease immunogenicity, and suppress nonspecific binding to charged molecules [35–37]. Similar to our approach, Bannister et al. used PEGylated gold nanoparticles (GNPs) with DTX and radiotherapy as a therapeutic strategy rather than a drug delivery system [23]. In their approach, DTX redistributed GNPs closer to the nucleus of cancer cells, enhancing DTX double-stranded breaks during radiation.

In this study, DTX dose reduction was assessed by combining low DTX doses with LANT, and our results suggest that LANT improved the therapeutic efficacy of low DTX doses in vitro. LANT dose reduction was omitted from this study because our previous in vivo study showed that the effective LANT monotreatment dose significantly induced tumor regression by approximately 100% ($p < 0.0001$) with no observed toxicity or side effects [39]. The performance of LANT monotreatment inspired the exploration of combining LANT with DTX as a synergistic therapeutic approach to lower the effective DTX dose, minimize the side effects of DTX, and improve patient outcomes. Combining DTX + LANT increased the percentage of cell death by up to 3.4-fold and the efficacy of cell death up to 51.5% more than DTX monotreatment. The most effective treatment combinations consistently demonstrated a >80% dose reduction in DTX to achieve the same level of cell death as DTX alone. Our current results suggest that combining LANT with DTX may dramatically lower the dose necessary to achieve therapeutic efficacy. The scope of LANT is currently limited to a single, local treatment, and therefore, additional experimentation is needed to examine its potential application in recurrent and metastatic disease. Our future studies will address these limitations, validate our findings in vivo, and provide greater insight on the clinical implications of LANT and DTX combination treatment, including dose, side effects and administration routes.

4. Materials and Methods

4.1. Materials

Gold (III) chloride trihydrate ($HAuCl_4$), cetyltrimethylammonium bromide (CTAB), sodium borohydride ($NaBH_4$), silver nitrate ($AgNO_3$), L-ascorbic acid, potassium carbonate (K_2CO_3), and dimethyl sulfoxide (DMSO) were purchased from Sigma-Aldrich (St. Louis, MO, USA). Thiol-terminated methoxy poly-(ethylene glycol) (mPEG-SH, MW 5000 K) and DTX were purchased from Creative PEGWorks (Winston-Salem, NC) and Selleck Chemicals (ImClone Systems, New York, NY, USA), respectively. UltraPure water (18 MΩ) was used for gold nanorod preparation.

4.2. Preparation of AuNRs

AuNRs were prepared using seed-mediated growth, PEGylated, and characterized according to the gold nanorods fabrication and characterization methods previously reported [40]. Briefly, PEGylated AuNRs solution was centrifuged at 7600× *g* for 20 min at 25 °C and re-dispersed in deionized water to remove excess CTAB and non-specifically bound mPEG-SH molecules. The maximum peak of plasmon resonance absorption for different batches of AuNRs averaged at λ = 808 nm as measured by a UV/VIS spectrophotometer UV5 Nano (Mettler Toledo, LLC, Columbus, OH, USA). The shape and size of AuNRs were confirmed by an aberration-corrected dedicated Scanning Transmission Electron Microscope HF2000 STEM (Hitachi High-Tech Corporation, Tokyo, Japan). The AuNRs were approximately 40 by 10 nm, thus providing the aspect ratio, R = 4. The concentration of AuNRs was calculated using Beer–Lambert Law based on the previously determined molar absorptivity, $\varepsilon = 5 \times 10^9$ L × mol^{-1} × cm^{-1} for 808 nm and aspect ratio, R = 4 [50].

4.3. Cell Lines

Human HNSCC cell lines, Detroit 562 (pharynx), FaDu (hypopharynx), and CAL 27 (tongue), were purchased from the American Type Culture Collection (ATCC, Manassas, VA, USA). All are tumorigenic and can translate to in vivo studies using xenografted HNSCC mice models. Upon receiving the cell lines from ATCC, the passage number was set at one, and passage 3–7 of each cell line was used. Cells tested negative for mycoplasma. Cells were cultured in Dulbecco's Modified Eagle Medium containing 10% *v*/*v* heat-inactivated fetal bovine serum, supplemented with 4.5 g/L glucose, L-glutamine, and penicillin-streptomycin, and incubated at 37 °C with 5% CO_2.

4.4. Cell Death by LANT and DTX Monotreatments

For LANT monotreatment in vitro, a total of 6×10^4 cells/well were seeded in 96-well culture plates and treated at approximately 100% confluence. The cell number per well was 6-times more than for DTX monotreatment to prepare a more than 99% confluent cell layer after seeding because the LANT effect is more immediate than anticancer drug cytotoxicity. AuNRs using a dose escalation of 0–25 nM in 25 µL were added to each well and immediately exposed to a diode near-infrared (NIR) laser (Information Unlimited, Amherst, NH, USA) with 808 nm wavelength at 1.875 W/cm^2 (spot size around 4×4 mm^2) for 4 min at room temperature. The 4-min duration of laser exposure in vitro was determined in our prior work [40] and used to maintain methodological consistency. Within 5 min after laser excitation of AuNRs, the percentage of cell death was determined by the PrestoBlue Assay according to the manufacturer's instructions. The percentage of cell death was calculated by subtracting the percentage of cell viability from 100% (see formula below).

$$\begin{aligned} \%\text{ of cell death} = {} & 100 - \%\text{ cell viability} \\ = {} & 100 - \frac{(\text{fluorescence of sample} - \text{fluorescence of blank})}{(\text{fluorescence of control} - \text{fluorescence of blank})} \\ & \times 100 \end{aligned}$$

For DTX monotreatment, cells were seeded in 96-wells plates at 1×10^4 cells/well and allowed to adhere overnight. The culture medium was then replaced with a fresh medium containing DTX at various concentrations, 0.0025–20 nM, and cells were incubated at 37 °C for 48 h. A pilot study was used to determine the ideal exposure time to DTX. The exposure for 24 h was insufficient to induce cell death, and 72 h exposure induced too much cytotoxicity to distinguish the impact of LANT from the anticancer activity of the respective DTX dose. Therefore, 48 h exposure was selected as the ideal DTX treatment time for the combination with LANT. The percentage of cell death was determined by the PrestoBlue Assay. The half-effective concentrations (EC50) of DTX and LANT for the 3 HNSCC cell lines were calculated with the IC50 calculator provided by AAT Bioquest® and the Four-Parameter Logistic (4PL) model [43].

4.5. Combination of DTX and LANT In Vitro

HNSCC cells were treated with the combination of DTX and LANT according to the methods used in our previous study [42], adapted as follows: HNSCC cell lines were seeded in 96-well plates at 1×10^4 cells/well and allowed to adhere overnight. The cell number was the same as that for DTX monotreatment. The cells were incubated with fresh medium containing DTX at two concentrations (0.5 or 1 nM) at 37 °C for 48 h. Immediately after the 48-h incubation, the DTX-medium was removed, and the cells were washed with PBS once. Then 25 µL of AuNRs in PBS at 2.5 or 5 nM were added onto the DTX-treated cells and exposed to 4 min of 808 nm wavelength NIR irradiation at 1.875 W/cm^2. As described above, the final percentage of cell death induced by the DTX + LANT combination treatment was evaluated using the PrestoBlue Assay immediately after LANT treatment. Each treatment combination was performed in quadruplicate (n = 4), and the results are expressed as the mean ± standard deviation.

The dose reduction realized by combining DTX with LANT was estimated by comparing the combination treatment to the monotreatment using the 4PL model equation for each cell line, as shown below.

For Detroit 562,

$$y = 5.955 + \frac{(100.971 - 5.955)}{1 + \left(\frac{x}{1.094}\right)^{-0.967}} \quad (1)$$

For FaDu,

$$y = 3.854 + \frac{(95.612 - 3.854)}{1 + \left(\frac{x}{0.895}\right)^{-1.197}} \quad (2)$$

For CAL 27,

$$y = 2.043 + \frac{(101.778 - 2.043)}{1 + \left(\frac{x}{1.238}\right)^{-1.842}} \quad (3)$$

To determine the percentage of cell death that is in common with both the DTX monotreatment and DTX + LANT combination treatment, we substituted the cell death percentage in the combination treatment obtained from in vitro data for y in Equations (1)–(3) for each cell line and then solved for x to calculate the corresponding DTX monotreatment dose.

4.6. Statistical Power and Analysis

The total sample size for the regression analyses was 72 (four observations per each of the six treatments (n = 6) and three cell lines). We assumed (1) an Ordinary Least Square multiple regression model with the treatment by cell lines as predictors, (2) an assumed R^2 value of 0.7 for the full model (proportion of variability in percent cell death explained by the treatment by cell combinations), (3) a differential effect in R^2 of 0.025 for each treatment by cell line combination, and (4) overall 0.05 significance level. Consequently, there is at least 90% power to detect a statistically significant difference between at least eight comparisons of DTX and LANT versus DTX monotreatment. Cell death percentages across the six treatment conditions, by cell line, were summarized by mean and standard deviations, median (min and max). The Linear Mixed Model (LMM) regression modeling approach with interaction (between treatment and cell lines) terms was used to compare the percentage of cell death between treatment combinations by cell lines. Multiple comparisons were adjusted using the Bonferroni correction, with an overall nominal statistical significance of α = 0.05. In other words, the synergy/interaction was evaluated using procedure MIXED in SAS, and our model incorporated interactions between treatment groups and cell lines. The algorithm underlying this model used additive effects, which took into account the hierarchal order of the magnitude of these effects. All of the iterative versions of the model applied the Bonferroni correction for multiple comparisons. No sigmoid (non-linear) feature for data was detected since the percent data lies between 17 and 95. However, given the bounded nature of the percent data (between 0 and 100), LMM results were also confirmed using a two-limit Tobit model [44]. The comparisons of interest are those between DTX monotreatment (i.e., 0.5 nM DTX and 1 nM DTX) and DTX and LANT combination treatment (i.e., 0.5 nM DTX + 2.5 nM LANT; 0.5 nM DTX + 5 nM LANT; 1 nM DTX + 2.5 nM LANT; and 1 nM DTX + 5 nM LANT). Summaries and differences were plotted using Boxplots. All analyses used SAS 9.4 and R statistical software (R Core Team, 2019).

Author Contributions: G.Y.L.: conceptualization, data curation, investigation, methodology, validation, visualization, writing—original manuscript preparation and revisions. M.M.: formal analysis. T.S.M.: writing—review and editing. N.C.S.: writing—review and editing. M.E.S.: writing—review and editing. C.E.F.: writing—review and editing. B.E.O.: writing—review and editing. M.B.C.: writing—original draft preparation. H.-N.G.: conceptualization (equal), data analysis, funding acquisition, methodology, project administration, resources, supervision, writing—original manuscript preparation and revisions. All authors have read and agreed to the published version of the manuscript.

Funding: The study was primarily supported by Award Number I01BX007080 from the Biomedical Laboratory Research and Development Service of the VA Office of Research and Development and partially supported by the National Center for Advancing Translational Sciences of the National Institutes of Health under Award Number UL1TR000454 and National Cancer Institute awards: P30CA013148, P50CA098252, U54CA118938, U54CA118623, and U54CA118948. The contents of this article are solely the responsibility of the authors and do not necessarily represent the official views of the funding agencies, VA or NIH.

Institutional Review Board Statement: Not applicable.

Informed Consent Statement: Not applicable.

Data Availability Statement: The datasets used or analyzed during the current study are available from the corresponding author on reasonable request.

Acknowledgments: The authors would like to thank the supporters and volunteers at the Ora Lee Smith Cancer Research Foundation for their endeavors to translate LANT from bench to bedside while making it affordable and accessible. This study was primarily supported by the Biomedical Laboratory Research and Development Service of the VA Office of Research and Development (I01BX007080), and partially supported by the National Center for Advancing Translational Sciences of the National Institutes of Health (UL1TR000454) and National Cancer Institute (grant numbers P30CA013148, P50CA098252, U54CA118938, U54CA118623, and U54CA118948). The authors disclose the following patent as a potential conflict of interest: Green, H.N. Photothermal nanostructures in tumor therapy. U.S. Patent No. US 9,827,441 B2. (Issued 28 November 2017).

Conflicts of Interest: The authors declare no conflict of interest.

References

1. Siegel, R.; Naishadham, D.; Jemal, A. Cancer statistics, 2013. *CA Cancer J. Clin.* **2013**, *63*, 11–30. [CrossRef] [PubMed]
2. Bray, F.; Ferlay, J.; Soerjomataram, I. Global cancer statistics 2018: GLOBOCAN estimates of incidence and mortality worldwide for 36 cancers in 185 countries. *CA Cancer J. Clin.* **2018**, *68*, 394–424. [CrossRef]
3. Blanchard, P.; Baujat, B.; Holostenco, V.; Bourredjem, A.; Baey, C.; Bourhis, J.; Pignon, J.-P. MACH-CH Collaborative group. Meta-analysis of chemotherapy in head and neck cancer (Mach-Nc): A comprehensive analysis by tumour site. *Radiother. Oncol.* **2011**, *100*, 33–40. [CrossRef]
4. Vigneswaran, N.; Williams, M.D. Epidemiologic trends in head and neck cancer and aids in diagnosis. *Oral Maxillofac. Surg. Clin. N. Am.* **2014**, *26*, 123–141. [CrossRef] [PubMed]
5. Marur, S.; Forastiere, A.A. Head and neck squamous cell carcinoma: Update on epidemiology, diagnosis, and treatment. *Mayo Clin. Proc.* **2016**, *91*, 386–396. [CrossRef] [PubMed]
6. Alsahafi, E.; Begg, K.; Amelio, I.; Raulf, N.; Lucarelli, P.; Sauter, T.; Tavassoli, M. Clinical update on head and neck cancer: Molecular biology and ongoing challenges. *Cell Death Dis.* **2019**, *10*, 1–17. [CrossRef]
7. Docetaxel—National Cancer Institute. Published 10 May 2006. Available online: https://www.cancer.gov/about-cancer/treatment/drugs/docetaxel (accessed on 2 March 2021).
8. Lyseng-Williamson, K.A.; Fenton, C. Docetaxel: A review of its use in metastatic breast cancer. *Drugs* **2005**, *65*, 2513–2531. [CrossRef]
9. McKeage, K. Docetaxel: A review of its use for the first-line treatment of advanced castration-resistant prostate cancer. *Drugs* **2012**, *72*, 1559–1577. [CrossRef] [PubMed]
10. Ho, M.Y.; Mackey, J.R. Presentation and management of docetaxel-related adverse effects in patients with breast cancer. *Cancer Manag. Res.* **2014**, *6*, 253–259. [CrossRef]
11. Valero, V. Docetaxel as single-agent therapy in metastatic breast cancer: Clinical efficacy. *Semin. Oncol.* **1997**, *24* (Suppl. S13), S13-11–S13-18.
12. Catimel, G.; Verweij, J.; Mattijssen, V.; Hanauske, A.; Piccart, M.; Wanders, J.; Franklin, H.; Le Bail, N.; Clavel, M.; Kaye, S.B.; et al. Docetaxel (Taxotere®): An active drug for the treatment of patients with advanced squamous cell carcinoma of the head and neck. *Ann. Oncol.* **1994**, *5*, 533–537. [CrossRef] [PubMed]
13. Colevas, A.D.; Posner, M.R. Docetaxel in head and neck cancer: A review. *Am. J. Clin. Oncol.* **1998**, *21*, 482–486. [CrossRef]
14. Couteau, C.; Chouaki, N.; Leyvraz, S.; Oulid-Aissa, D.; Lebecq, A.; Domenge, C.; Groult, V.; Bordessoule, S.; Janot, F.; De Forni, M.; et al. A phase II study of docetaxel in patients with metastatic squamous cell carcinoma of the head and neck. *Br. J. Cancer* **1999**, *81*, 457–462. [CrossRef] [PubMed]
15. Fernandes, K.A.; Felix, P.A. Persistent docetaxel-induced supravenous erythematous eruption. *An. Bras. Dermatol.* **2015**, *90*, 728–730. [CrossRef] [PubMed]
16. Cortes, J.E.; Pazdur, R. Docetaxel. *J. Clin. Oncol.* **1995**, *13*, 2643–2655. [CrossRef]
17. Trudeau, M.E. Docetaxel: A review of its pharmacology and clinical activity. *Can. J. Oncol.* **1996**, *6*, 443–457.

18. Bernier, J.; Vrieling, C. Docetaxel in the management of patients with head and neck squamous cell carcinoma. *Expert Rev. Anticancer Ther.* **2008**, *8*, 1023–1032. [CrossRef]
19. Haddad, R.; Posner, M.; Hitt, R.; Cohen, E.; Schulten, J.; Lefebvre, J.-L.; Vermorken, J. Induction chemotherapy in locally advanced squamous cell carcinoma of the head and neck: Role, controversy, and future directions. *Ann. Oncol.* **2018**, *29*, 1130–1140. [CrossRef]
20. DailyMed—DOCETAXEL Injection, Solution. Available online: https://dailymed.nlm.nih.gov/dailymed/drugInfo.cfm?setid=3104aab1-cd6e-4ad2-8e0a-286a0c5d1940#S5.1 (accessed on 2 March 2021).
21. Albers, A.E.; Grabow, R.; Qian, X.; Jumah, M.D.; Hofmann, V.M.; Krannich, A.; Pecher, G. Efficacy and toxicity of docetaxel combination chemotherapy for advanced squamous cell cancer of the head and neck. *Mol. Clin. Oncol.* **2017**, *7*, 151–157. [CrossRef]
22. Galletti, E.; Magnani, M.; Renzulli, M.L.; Botta, M. Paclitaxel And Docetaxel Resistance: Molecular Mechanisms and Development of New Generation Taxanes. *ChemMedChem* **2007**, *2*, 920–942. [CrossRef] [PubMed]
23. Bannister, A.H.; Bromma, K.; Sung, W.; Monica, M.; Cicon, L.; Howard, P.; Chow, R.L.; Schuemann, J.; Chithrani, D.B. Modulation of nanoparticle uptake, intracellular distribution, and retention with docetaxel to enhance radiotherapy. *Br. J. Radiol.* **2020**, *93*, 20190742. [CrossRef] [PubMed]
24. Tran, P.; Duan, W.; Lee, B.-J.; Tran, T.T. Nanogels for Skin Cancer Therapy via Transdermal Delivery: Current Designs. *Curr. Drug Metab.* **2019**, *20*, 575–582. [CrossRef]
25. Her, S.; Jaffray, D.A.; Allen, C. Gold nanoparticles for applications in cancer radiotherapy: Mechanisms and recent advancements. *Adv. Drug Deliv. Rev.* **2017**, *109*, 84–101. [CrossRef]
26. Essawy, M.M.; El-Sheikh, S.M.; Raslan, H.S.; Ramadan, H.S.; Kang, B.; Talaat, I.M.; Afifi, M.M. Function of gold nanoparticles in oral cancer beyond drug delivery: Implications in cell apoptosis. *Oral Dis.* **2021**, *27*, 251–265. [CrossRef]
27. Choi, Y.J.; Kim, Y.J.; Lee, J.W.; Lee, Y.; Lee, S.; Lim, Y.-B.; Chung, H.W. Cytotoxicity and genotoxicity induced by photothermal effects of colloidal gold nanorods. *J. Nanosci. Nanotechnol.* **2013**, *13*, 4437–4445. [CrossRef]
28. Zhou, B.; Song, J.; Wang, M.; Wang, X.; Wang, J.; Howard, E.W.; Zhou, F.; Qu, J.; Chen, W.R. BSA-bioinspired gold nanorods loaded with immunoadjuvant for the treatment of melanoma by combined photothermal therapy and immunotherapy. *Nanoscale* **2018**, *10*, 21640–21647. [CrossRef]
29. Hijaz, M.; Das, S.; Mert, I.; Gupta, A.; Al-Wahab, Z.; Tebbe, C.; Dar, S.; Chhina, J.; Giri, S.; Munkarah, A.; et al. Folic acid tagged nanoceria as a novel therapeutic agent in ovarian cancer. *BMC Cancer* **2016**, *16*, 1–14. [CrossRef]
30. Li, H.; Qu, X.; Qian, W.; Song, Y.; Wang, C.; Liu, W. Andrographolide-loaded solid lipid nanoparticles enhance anti-cancer activity against head and neck cancer and precancerous cells. *Oral Dis.* **2020**. [CrossRef] [PubMed]
31. Sun, B.; Feng, S.S. Trastuzumab-functionalized nanoparticles of biodegradable copolymers for targeted delivery of docetaxel. *Nanomedicine* **2009**, *4*, 431–445. [CrossRef]
32. Tang, X.; Wang, G.; Shi, R.; Jiang, K.; Meng, L.; Ren, H.; Wu, J.; Hu, Y. Enhanced tolerance and antitumor efficacy by docetaxel-loaded albumin nanoparticles. *Drug Deliv.* **2015**, *23*, 2686–2696. [CrossRef] [PubMed]
33. Bowerman, C.J.; Byrne, J.D.; Chu, K.S.; Schorzman, A.N.; Keeler, A.W.; Sherwood, C.A.; Perry, J.L.; Luft, J.C.; Darr, D.B.; Deal, A.M.; et al. Docetaxel-Loaded PLGA Nanoparticles Improve Efficacy in Taxane-Resistant Triple-Negative Breast Cancer. *Nano Lett.* **2017**, *17*, 242–248. [CrossRef] [PubMed]
34. Choudhury, H.; Gorain, B.; Pandey, M.; Kumbhar, S.A.; Tekade, R.K.; Iyer, A.K.; Kesharwani, P. Recent advances in TPGS-based nanoparticles of docetaxel for improved chemotherapy. *Int. J. Pharm.* **2017**, *529*, 506–522. [CrossRef] [PubMed]
35. Wan, J.; Ma, X.; Xu, D.; Yang, B.; Yang, S.; Han, S. Docetaxel-decorated anticancer drug and gold nanoparticles encapsulated apatite carrier for the treatment of liver cancer. *J. Photochem. Photobiol. B Biol.* **2018**, *185*, 73–79. [CrossRef]
36. Chi, C.; Li, F.; Liu, H.; Feng, S.; Zhang, Y.; Zhou, D.; Zhang, R. Docetaxel-loaded biomimetic nanoparticles for targeted lung cancer therapy in vivo. *J. Nanoparticle Res.* **2019**, *21*, 144. [CrossRef]
37. Ahmad, T.; Sarwar, R.; Iqbal, A.; Bashir, U.; Farooq, U.; Halim, S.A.; Khan, A.; Al-Harrasi, A. Recent advances in combinatorial cancer therapy via multifunctionalized gold nanoparticles. *Nanomedicine* **2020**, *15*, 1221–1237. [CrossRef]
38. Popp, M.K.; Oubou, I.; Shepherd, C.; Nager, Z.; Anderson, C.; Pagliaro, L. Photothermal Therapy Using Gold Nanorods and Near-Infrared Light in a Murine Melanoma Model Increases Survival and Decreases Tumor Volume. *J. Nanomater.* **2014**, *2014*, 1–8. [CrossRef]
39. Green, H.; Crockett, S.; Martyshkin, D.; Singh, K.; Grizzle, W.; Rosenthal, E.; Mirov, S. A histological evaluation and in vivo assessment of intratumoral near infrared photothermal nanotherapy-induced tumor regression. *Int. J. Nanomed.* **2014**, *9*, 5093–5102. [CrossRef]
40. Green, H.N.; Martyshkin, D.V.; Rosenthal, E.L.; Mirov, S.B. *A Minimally Invasive Multifunctional Nanoscale System for Selective Targeting, Imaging, and NIR Photothermal Therapy of Malignant Tumors*; Achilefu, S., Raghavachari, R., Eds.; SPIE BiOs (Proceeding): San Francisco, CA, USA, 10 February 2011; p. 79100B. [CrossRef]
41. Lee, G.Y.; Mubasher, M.; Pollack, B.P.; McKenzie, T.; Cothran, M.B.; Green, H.N. Combination paclitaxel and Laser-Activated NanoTherapy for inducing cell death in head and neck squamous cell carcinoma. *J. Nanomed. Nanotech.* **2021**, *12*, 557.
42. Lee, G.Y.; Perez, S.M.; Singh, K.P.; Green, H.N. Cisplatin combined with laser-activated nanotherapy as an adjuvant therapy for head and neck cancer. *Int. J. Oncol.* **2020**, *57*, 1169–1178. [CrossRef]
43. Sebaugh, J.L. Guidelines for accurate EC50/IC50 estimation. *Pharm. Stat.* **2011**, *10*, 128–134. [CrossRef]

44. Long, J.S. *Regression Models for Categorical and Limited Dependent Variables*; Advanced quantitative techniques in the social sciences; Sage Publications: Thousand Oaks, CA, USA, 1997.
45. Figgitt, D.P.; Wiseman, L.R. Docetaxel: An update of its use in advanced breast cancer. *Drugs* **2000**, *59*, 621–651. [CrossRef]
46. Yao, M.; Galanopoulos, N.; Lavertu, P.; Fu, P.; Gibson, M.; Argiris, A.; Rezaee, R.; Zender, C.; Wasman, J.; Machtay, M.; et al. Phase II study of bevacizumab in combination with docetaxel and radiation in locally advanced squamous cell carcinoma of the head and neck. *Head Neck* **2014**, *37*, 1665–1671. [CrossRef]
47. Elbehi, A.M.; Anu, R.; Ekine-Afolabi, B.; Cash, E. Emerging role of immune checkpoint inhibitors and predictive biomarkers in head and neck cancers. *Oral Oncol.* **2020**, *109*, 104977. [CrossRef] [PubMed]
48. Adkins, D.; Ley, J.; Atiq, O.; Powell, S.; Spanos, W.C.; Gitau, M.; Rigden, C.; Palka, K.; Liu, J.; Oppelt, P. Nanoparticle albumin-bound paclitaxel with cetuximab and carboplatin as first-line therapy for recurrent or metastatic head and neck cancer: A single-arm, multicenter, phase 2 trial. *Oral Oncol.* **2021**, *115*, 105173. [CrossRef]
49. Marcazzan, S.; Varoni, E.M.; Blanco, E.; Lodi, G.; Ferrari, M. Nanomedicine, an emerging therapeutic strategy for oral cancer therapy. *Oral Oncol.* **2018**, *76*, 1–7. [CrossRef]
50. Link, S.; El-Sayed, M.A. Simulation of the optical absorption spectra of gold nanorods as a function of their aspect ratio and the effect of the medium dielectric constant. *J. Phys. Chem. B* **2005**, *109*, 10531–10532. [CrossRef]